

BPDA2d—a 2D global optimization-based Bayesian peptide detection algorithm for liquid chromatograph–mass spectrometry

Youting Sun¹, Jianqiu Zhang^{2,*}, Ulisses Braga-Neto¹ and Edward R. Dougherty^{1,3,4,*}

¹Department of Electrical Engineering, Texas A&M University, College Station, TX 77843, ²Department of Electrical Engineering, University of Texas at San Antonio, San Antonio, TX 78249, ³Computational Biology Division, Translational Genomics Research Institution, Phoenix, AZ 85004 and ⁴Department of Bioinformatics and Computational Biology, University of Texas M.D. Anderson Cancer Center, Houston, TX 77030, USA

Associate Editor: John Quackenbush

ABSTRACT

Motivation: Peptide detection is a crucial step in mass spectrometry (MS) based proteomics. Most existing algorithms are based upon greedy isotope template matching and thus may be prone to error propagation and ineffective to detect overlapping peptides. In addition, existing algorithms usually work at different charge states separately, isolating useful information that can be drawn from other charge states, which may lead to poor detection of low abundance peptides.

Results: BPDA2d models spectra as a mixture of candidate peptide signals and systematically evaluates all possible combinations of possible peptide candidates to interpret the given spectra. For each candidate, BPDA2d takes into account its elution profile, charge state distribution and isotope pattern, and it combines all evidence to infer the candidate's signal and existence probability. By piecing all evidence together—especially by deriving information across charge states—low abundance peptides can be better identified and peptide detection rates can be improved. Instead of local template matching, BPDA2d performs global optimization for all candidates and systematically optimizes their signals. Since BPDA2d looks for the optimal among all possible interpretations of the given spectra, it has the capability in handling complex spectra where features overlap. BPDA2d estimates the posterior existence probability of detected peptides, which can be directly used for probability-based evaluation in subsequent processing steps. Our experiments indicate that BPDA2d outperforms state-of-the-art detection methods on both simulated data and real liquid chromatography–mass spectrometry data, according to sensitivity and detection accuracy.

Availability: The BPDA2d software package is available at <http://gsp.tamu.edu/Publications/supplementary/sun11a/>

Contact: michelle.zhang@utsa.edu; edward@ece.tamu.edu

Supplementary information: Supplementary data are available at *Bioinformatics* online.

Received on July 28, 2011; revised on November 12, 2011; accepted on November 30, 2011

1 INTRODUCTION

Liquid chromatography coupled to mass spectrometry (LC–MS) is widely used for large-scale protein profiling of complex biological

samples. In a typical LC–MS experiment, peptides from digested protein mixture go through an LC column with different speeds depending on their physicochemical properties. Eluent from the chromatography is ionized and analyzed by mass spectrometer, which measures ions according to their mass-to-charge (m/z) ratios. The resulting LC–MS dataset usually contains hundreds to thousands of mass spectra indexed by the LC retention time.

Analysis of LC–MS experiments by computational methods is challenged by the huge data size and rich information contained, and moreover complicated by several facts including: (i) proteins contained in complex samples such as plasma and tissue extracts have a wide dynamic concentration range (e.g. 10 orders of magnitude), plus peptides differ in ionization efficiencies, which means that the observed peptide signal from MS data may also have a wide dynamic range. While high abundance peptides are relatively easy to be identified, low abundance peptides/proteins, which are often of more biological importance, are likely to be buried under noise or interfering signals and thus hard to be detected (Li *et al.*, 2005). (ii) The shape of peptide chromatographic peaks is not well predicted (Schulz-Trieglaff *et al.*, 2008). Due to experiment settings and the nature of the analytes, asymmetric shape or plateaus of chromatographic peaks may be observed, which requires designed detection algorithms to be robust in tracking signals from various peptide species and be adaptable across experiments. (iii) One peptide can be multiply charged and can register a group of isotopic peaks at each charge state. Correctly identifying all the peaks and assigning them to the right peptide is a non-trivial task. (iv) The signal density can be very high even in high-resolution LC–MS data and overlapping peptide peaks are commonly observed, the detection of which is very challenging.

Accurate identification and quantification of proteins is essential for biomarker discovery, drug development and disease classification (Frank *et al.*, 2003). Fragmentation spectra produced by tandem mass spectrometry (MS2) are frequently used by popular software such as SEQUEST and Mascot (Perkins *et al.*, 1999) for database searching to give peptide identifications. However only a small percentage of peptides present in the sample get selected for fragmentation analysis and of these selected peptides even fewer can be correctly identified by database searching due to spectra matching ambiguity or co-eluting precursor ions (Nesvizhskii *et al.*, 2006). Furthermore, quantitation of peptide abundance based on MS2 spectra counting is very rough, and highly variable especially for low abundance peptides (Bantscheff *et al.*, 2007). [Though by using well-established stable isotope labeling approaches such as

*To whom correspondence should be addressed.

tandem mass tags, the relative abundance of analytes in different samples can be accurately determined (Domon *et al.*, 2006).] Therefore, many algorithms for peptide detection are developed to use MS1 information directly, and thus have the potential to identify more peptides. Such algorithms can be mainly divided into two categories: 1D algorithms [e.g. NITPICK (Renard *et al.*, 2008), Decon2LS (Jaitly *et al.*, 2009), Hardklör (Hoopmann *et al.*, 2007) and BPDA (Sun *et al.*, 2010)] which perform peak picking, deisotoping and charge state assignment on a scan-to-scan basis, and 2D algorithms [e.g. MZmine (Katajamaa *et al.*, 2005), SpecArray (Li *et al.*, 2005), msInspect (Bellew *et al.*, 2006), SuperHirn (Mueller *et al.*, 2007), VIPER (Monroe *et al.*, 2007), MaxQuant (Cox *et al.*, 2008) and OpenMS (Sturm *et al.*, 2008)] which capture the 2D nature of LC–MS data and utilize information from both the mass-to-charge and retention time (RT) dimensions for peptide detection. 2D algorithms appear to be more promising in handling LC–MS data. Regardless of category, most of the aforementioned algorithms are grounded on the idea of greedy template matching. The templates used are often based on theoretic isotope patterns calculated from peptide masses (Rockwood *et al.*, 1995). If an observed group of peaks matches the proposed template well—the quality of the match is usually assessed by a fitting score—it will be reported as a feature and then subtracted from the spectra. The matching and subtraction process goes on until no more matches can be found. The major problem with greedy template matching is that it may be ineffective to detect overlapping peptides. In the case of overlapping (e.g. one doubly charged peptide can overlap with a singly charged peptide of half the mass given that the two elute from chromatography at a similar time), if the peak group of one peptide is incorrectly matched and subtracted, the rest of the overlapping peptides cannot be detected correctly using the remaining signal, which may result in error propagation. Besides, each template is aimed at matching isotopic peaks of one single peptide, and thus is likely to be different from the observed overlapping peaks, which renders a poor match and reduces the sensitivities of these algorithms. Alternatives to greedy template matching-based approaches include 1D algorithms such as NITPICK, which is based on LARS regression; Hardklör, which approximates an isotope peak cluster by a set of average models (Senko *et al.*, 1995); and BPDA, which carries out global optimization instead of sequential template matching. They also include 2D algorithms such as MaxQuant, which mainly relies on the distance among isotope peaks and the correlation between isotope labeled (SILAC) pairs to detect and quantify peptides in SILAC-proteome experiments.

We present BPDA2d, a 2D Bayesian peptide detection algorithm and an extension of BPDA, to process high-resolution LC–MS data more efficiently. BPDA2d shares the core idea with BPDA, which is to systematically evaluate all possible combinations of peptide candidates (originated from well-defined signal peaks) for spectra interpretation, and to optimize all peptide signals in order to minimize the mean squared error (MSE) between inferred and observed spectra. The outputs include peptide monoisotopic mass, RT, abundance, existence probability, etc. BPDA2d essentially differs from BPDA by explicitly exploiting information residing in the RT dimension to analyze spectra and detect peptides. While BPDA only models peptide signals along the m/z dimension, BPDA2d models the spectra from both m/z and RT dimensions, thereby capturing and fitting the properties of LC–MS data better.

BPDA2d offers following advantages over conventional methods:

- (i) BPDA2d carries out global optimization instead of local template matching. It is ‘global’ in two senses: first, for the detection of one peptide candidate, BPDA2d extracts all relevant information and observations (including isotopic peaks, charge state distributions and LC elution peaks) that span all over the m/z -RT space, and pieces all evidence together to infer the candidate’s existence probability. As a result, low abundance peptides can be better identified. In contrast, existing algorithms often perform peptide deisotoping at a single charge state (Bellew *et al.*, 2006; Hoopmann *et al.*, 2007; Jaitly *et al.*, 2009; Katajamaa *et al.*, 2005; Li *et al.*, 2005; Mueller *et al.*, 2007; Sturm *et al.*, 2008), isolating useful information that can be drawn from other charge states. While high abundance charge states may be correctly detected, low abundance charge states might be missed or wrongly assigned, rendering low sensitivity results in peptide identification and inaccuracy in peptide quantification. Additional benefits of collating all charge states are discussed in Dijkstra *et al.* (2009). (Though their method requires the peak clusters at various charge states to have a moderate correlation, and thus may not work efficiently if the shape of the peak cluster at any charge state differs from other charge states due to the presence of interfering peptides.) Second, BPDA2d performs global optimization for all candidates and simultaneously finds their best fitting signals. Since BPDA2d looks for the optimal among all possible interpretations of the MS spectra, the procedure is thus systematic. In contrast, greedy template matching-based methods detect peptides one by one in a greedy manner, which prevents them from evaluating all potential interpretations of the given spectra and may lead to poor detection of overlapping peptides (See Section 3). Therefore, the results are often suboptimal.
- (ii) BPDA2d provides existence probabilities for all the candidates considered, as opposed to the fitting scores generally provided by greedy template matching methods. The metrics used for fitting score calculation may be heuristic [e.g. KL distance (Bellew *et al.*, 2006)]. In addition, the range of the fitting score may vary from experiment to experiment, making it hard for the end user to interpret and to select a proper threshold to filter out low-quality features. On the contrary, existence probabilities given by BPDA2d are derived based on a solid statistical framework and can be directly used for probability-based evaluation—similar to PeptideProphet (Keller *et al.*, 2002) which is a popular software used for LC–MS/MS peptide identification.
- (iii) BPDA2d makes little assumptions about the shape of elution peaks. A non-parametric approach is used to model peptide elution peaks and the model is derived from observations as opposed to employing any pre-assumed peak shape as in Leptos *et al.* (2006); Sturm *et al.* (2008). Therefore, BPDA2d is more effective in tracking signals from various peptide species and more adaptable across experiments.
- (iv) Most parameters in the proposed method possess a clear physical meaning as they come directly from observations of the mass spectra. In contrast, many other approaches

require selection of numerous non-intuitive parameters, such as wavelet functions and coefficients (Morris *et al.*, 2005).

2 METHODS

We first preprocess the spectra to remove baseline, filter noise, detect peaks in the m/z -RT plane, and generate a list of peptide candidates annotated by mass and RT. Then BPDA2d is applied based on the developed MS model to infer the best fitting peptide signals of observed spectra, the results being peptide monoisotopic mass, RT, abundance, existence probability, etc. Details of preprocessing steps, proposed MS model and BPDA2d algorithm are described in the following subsections.

2.1 Spectra preprocessing and obtaining peptide candidates

Non-flat baselines are often observed in mass spectra. Their presence can distort the true signal pattern. Thus, the baseline of each MS scan is first identified as the running minima along the m/z axis using a window size of 4 Da (a tunable parameter), and subtracted from the scan. Then each scan is smoothed by the LOWESS regression method (Matlab `mslowess` function <http://www.mathworks.com/help/toolbox/bioinfo/ref/mslowess.html>) with Gaussian kernel and a span of nine consecutive points.

The next step is 1D peak detection along the m/z axis. We followed the approach implemented in the Matlab `mspeaks` function <http://www.mathworks.com/access/helpdesk/help/toolbox/bioinfo/ref/mspeaks.html>. Specifically, in each smoothed MS scan, local maxima are first identified as putative peak locations. Then peaks are filtered based on their intensities and signal to noise ratios (defined as the local maximum divided by the minimum of the two neighboring local minima), and peaks that are too close to each other (might occur due to over-segmentation) are joined into a single one. The thresholds used for intensity and over-segmentation filters, τ_{intn} and τ_{seg} , respectively, are automatically determined depending on the characteristic of each input MS scan as below:

$$\tau_{\text{intn}} = \text{mean}(\text{intn}) + \text{sd}(\text{intn}),$$

$$\tau_{\text{seg}} = \min\left(\frac{200}{\text{resolution}}, 7 \times \text{lower } 10\% \text{ quantile of the space}\right)$$

between neighboring m/z values).

And the SNR threshold is a tunable parameter with default value 3.

Next, the detected 1D peaks in adjacent spectra are connected along the RT dimension: 1D peaks are first sorted by their centroid m/z positions, and then divided into disjoint subsets, in which the maximal m/z distance between two 1D peaks is less than twice the smallest m/z in the subset times Δm (a user defined mass error in ppm). For each subset, the peaks are then sorted/connected according to their RT positions (if multiple peaks have the same RT, only the one with the largest intensity is retained). Next, the connected 1D peaks are split at RT gaps (a tunable parameter), and the resulting so-called elution peaks are smoothed by the LOWESS regression method with a ± 3 scan width. The elution peaks could be multimodal, which may for instance be produced by two different peptides with partially overlapping elution peaks, or by isomers with variant post-translational modifications and thus different retention times. Multimodal elution peaks are split at local minima. A point is identified as a local minima/maxima if it is preceded by a local maxima/minima and is followed by a value greater/lower by 15% (the threshold is a user tunable parameter which should be comparable to the random intensity fluctuations of the instrument). Consequently, all elution peaks are now unimodal, which will be used to propose a list of peptide candidates in the next step. For each elution peak, its centroid position in the m/z axis is estimated as the average of the m/z values of the connected 1D peaks weighted by their intensities. This method enables very accurate mass estimation, as reported by Cox *et al.* (2008).

Now, considering one elution peak with centroid at m/z value d , we want to find out which peptide candidates can potentially produce this signal peak.

At least two conditions need to be satisfied. (i) The masses of such peptides should be restricted to the following set:

$$\{\text{mass} \mid \text{mass} = i(d - m_{pc}) - jm_{nt}, \\ i = 1, 2, \dots, cs, j = 0, 1, \dots, iso\}, \quad (1)$$

where $mass$ is the mass of such a candidate, m_{pc} is the mass of one positive charge and m_{nt} is the mass shift caused by addition of one neutron. Due to mass defect, the mass shift varies for different elements. We approximate m_{nt} using the mass shift from ^{13}C to ^{12}C , which is 1.0034, since Carbon contributes most to the isotope patterns. But m_{nt} is a user accessible parameter whose value can be changed as needed. The parameters cs and iso are user-defined maximal numbers of considered charge states and isotopic positions, respectively. (ii) The shapes of such candidates' elution peaks should resemble the aforementioned elution peak with centroid d (hereafter referred to as the 'source' elution peak). But in the presence of scan noise, missing values or overlapping peptide signals, the actual shapes of candidates' elution peaks can be quite different from the observed shape of the source peak. Thus, in order to estimate candidates' elution peaks more accurately, other elution peaks which can be produced by such candidates need to be taken into account. In more detail, assume the source elution peak has given rise to a candidate with mass value $mass_k$ taken from the set defined in Equation (1). Then, theoretically, this candidate can generate a set of elution peaks with centroids given by

$$\alpha_{k,ij} = \frac{mass_k + im_{pc} + jm_{nt}}{i}, \quad (2) \\ i = 1, 2, \dots, cs, j = 0, 1, \dots, iso,$$

where $\alpha_{k,ij}$ is the theoretic centroid (m/z value) of the elution peak generated by candidate $mass_k$ at charge state i and isotopic number j . In theory, the set of elution peaks generated by this very candidate should have the same shape (up to a multiplicative constant). Therefore, we search in the previous detected elution peaks for those whose centroids are coincident with the values given by Equation (2) (within Δ_m) and have correlation > 0.6 with the source elution peak, since these elution peaks can serve as extra evidence to infer the candidate's real elution peak. Finally the candidate's elution peak is estimated by taking the average of all identified elution peaks weighted by the mean intensity of each elution peak involved in the calculation. The candidate's elution profile is then obtained by normalizing its elution peak by the apex, and the corresponding RT of the apex is taken as the candidate's RT. It is worth to mention that we do not assume any particular shape for candidates' elution profiles, but instead estimate them from relevant observations. Due to heterogeneity of peptides and fluctuations in liquid chromatography, this approach is more robust in the presence of noise and more adaptable across analysis platforms compared to using any pre-defined model (Leptos *et al.*, 2006; Sturm *et al.*, 2008).

As can be seen from Equation (1), each detected elution peak gives rise to $cs \times (iso + 1)$ different peptide candidates whose elution profiles have been estimated in the previous step, but it does not follow that all these candidates really exist in the sample. Therefore, our primary goal in peptide detection is to find the existence probability of each peptide candidate. Also note that the total number of candidates should be less than or equal to $cs \times (iso + 1) \times$ (number of detected elution peaks), as it is possible that multiple elution peaks yield the same candidate. It is worth to mention that the way candidates are generated in BPDA2d is fundamentally different from that in BPDA, as additional information carried by elution peaks is utilized. Candidates are now associated with elution profiles in addition to mass values.

2.2 Modeling the mass spectra

We propose a complete model to capture the specific properties of peptides and mass spectra over the entire m/z -RT plane.

Suppose N peptide candidates are obtained from the observed spectra using methods described in the previous section. Each candidate can generate a series of elution peaks over different charge states, and at each charge state

several isotopic peaks can be registered. Hence, the signal generated by the k -th peptide candidate is modeled by Equation (3), in which i and j represent the charge state and the isotopic position of the candidate, respectively. The baseline removed and smoothed spectra (see the previous section for details) are a mixture of signals generated by N peptide candidates plus Gaussian random noise, which are modeled by Equation (4):

$$g_k(x_m, t) = \sum_{i=1}^{cs} \sum_{j=0}^{iso} c_{k,ij} I_k(t) I_{x_m=\alpha_{k,ij}}, \quad (3)$$

$$\begin{aligned} y(x_m, t) &= \sum_{k=1}^N \lambda_k g_k(x_m, t) + \epsilon(t) \\ &= \sum_{k=1}^N \lambda_k \sum_{i=1}^{cs} \sum_{j=0}^{iso} c_{k,ij} I_k(t) I_{x_m=\alpha_{k,ij}} + \epsilon(t), \end{aligned} \quad (4)$$

$$m = 1, 2, \dots, M, t = 1, 2, \dots, T.$$

In the above two equations, x_m is the m -th mass-to-charge ratio in the signal region, i.e. $x_m \in \{m/z \text{ values of detected elution peaks}\} \cup \{m/z \text{ values of all candidates' theoretic peaks}\}$, t indexes spectra, M and T are the total number of m/z values and spectra, respectively, $y(x_m, t)$ represents the intensity at point (x_m, t) , I is an indicator function, $I_A = 1$ if $A \neq \emptyset$, $I_A = 0$ otherwise, and the noise term $\epsilon(t)$ follows a Gaussian distribution with zero mean and SD $\sigma(t)$, which is generally a good model for thermal noise in electrical instruments. The value of $\sigma(t)$ can be approximated by the SD of the background region in the t -th scan. The parameters of the k -th candidate, namely, $\alpha_{k,ij}$, $I_k(t)$, λ_k and $c_{k,ij}$, are discussed in detail below:

- $\alpha_{k,ij}$ is the theoretic centroid position (in the m/z axis) of the elution peak generated by candidate k , at charge state i and isotopic number j , the value of which is given by Equation (2).
- $I_k(t)$ is the normalized elution profile of the k -th peptide candidate, which is already obtained in previous section.
- λ_k is an indicator random variable, which is 1 if the k -th peptide candidate truly exists in the sample and 0 otherwise.
- $c_{k,ij}$ is the apex intensity of the elution peak generated by peptide k , at charge state i and isotopic number j .

In summary, the model considers peptides' elution peaks at different isotopic positions and charge states simultaneously, incorporating candidates' existence probabilities and spectra thermal noise.

2.3 Bayesian peptide detection

Let $\theta \triangleq \{\lambda_k, c_{k,ij}; k=1, \dots, N, i=1, \dots, cs, j=0, \dots, iso\}$ be the set of all unknown model parameters. The goal of our algorithm is to determine the value of θ based on the observed spectra vector $\mathbf{y} = [y(x_m, t); m=1, 2, \dots, M, t=1, 2, \dots, T]^T$. The λ_k values are of our prime interest in the peptide detection problem. For this purpose, we can use a Bayesian approach to first obtain the *a posteriori* probability (APP) of all the parameters, $P(\theta|\mathbf{y})$. Then the APPs $P(\lambda_k|\mathbf{y}), k=1, \dots, N$, can be obtained by integrating the joint posterior distribution $P(\theta|\mathbf{y})$ over all parameters except λ_k . Clearly, the calculation involves intricate high dimension integration. Besides, due to the highly non-linear nature of the data model, none of these desired APPs can be obtained analytically. To overcome the computational obstacle, we resort to the Gibbs sampling method (Geman *et al.*, 1984), which is a variant of the Markov Chain Monte Carlo approach (Robert *et al.*, 2004), to sample the model parameters.

Gibbs sampling iteratively sample a subset of parameters while fixing the rest at the sample values from the previous iteration. In other words, for the l -th parameter group θ_l , we sample from the conditional posterior distribution $P(\theta_l|\theta_{-l}, \mathbf{y})$, where $\theta_{-l} \triangleq \theta \setminus \theta_l$. After this sampling process iterates among the parameter groups for a sufficient number of cycles (which is referred to as the 'burn-in' period), convergence is reached. The samples collected afterwards are shown to be from the marginal posterior distribution $P(\theta_l|\mathbf{y})$, which is

independent of θ_{-l} , and thus these samples can be used to estimate the target parameters.

The Gibbs sampling process for the k -th peptide candidate and the derivations of the conditional posterior distributions of important model parameters are briefly summarized below. Detailed derivations can be found in Supplementary Material.

- Sample the apex vector $\mathbf{c}_k \triangleq [c_{k,ij}; i=1, \dots, cs, j=0, \dots, iso]^T$ for the k -th candidate

Apexes of all possible elution peaks (over different charge states and isotopic positions) of the k -th peptide candidate are included in \mathbf{c}_k and are sampled simultaneously from the conditional posterior distribution of \mathbf{c}_k , which, by the Bayesian principle, is proportional to the likelihood times the prior:

$$P(\mathbf{c}_k | \mathbf{y}, \theta_{-c_k}) \propto P(\mathbf{y} | \theta) P(\mathbf{c}_k), \quad (5)$$

where $\theta_{-c_k} \triangleq \theta \setminus \mathbf{c}_k$.

Derivations of the likelihood, the prior distribution [which makes use of the Averagine model (Senko *et al.*, 1995)] and the conditional posterior distribution of \mathbf{c}_k are given in the Supplementary Material.

- Sample the peptide existence indicator variable λ_k . The conditional posterior distribution of λ_k is given by

$$P(\lambda_k | \mathbf{y}, \theta_{-\lambda_k}) \propto p(\mathbf{y} | \lambda_k) p(\lambda_k) \quad (6)$$

where $\theta_{-\lambda_k} \triangleq \theta \setminus \lambda_k$.

Absence of prior knowledge about which peptide candidates are more likely to be present in the sample, a reasonable choice is a uniform prior for λ_k . However, we wish to be conservative regarding the existence of peptide candidates. The idea is that by including more candidates, it is possible to reduce the MSE between the inferred and the observed spectra, but at the same time the chances of overfitting increase as model complexity grows. Thus, a prior based on Bayesian information criterion (BIC) (Schwarz, 1978) is adopted to address overfitting by introducing a penalty term for the number of parameters of the model. The penalty only takes effect when inclusion of one peptide does little to improve the goodness of fit.

For Gibbs sampling, it is well known that the correlation between parameters can reduce sampling efficiency. Thus, we cluster peptide candidates which have large overlaps in both m/z and RT dimensions together. Candidates within one cluster have strong correlations among each other, and their indicator variables are sampled from the joint conditional posterior distribution. The iteration order also affects the performance. Therefore, peptide clusters are first sorted by their importance, which is defined as the maximal intensity of the peptides in the cluster. The iteration starts from the most significant cluster and continues to the next significant one. Our experimental results suggest that this scheme helps to reduce false positives and speed up convergence. The pseudocode of the entire Gibbs sampling process is given in Supplementary Material.

Samples taken after convergence can be used to estimate target parameters, so the existence probability of peptide k is calculated as $P(\lambda_k=1|\mathbf{y}) = \frac{1}{R-r_0+1} \sum_{r=r_0}^R \lambda_k^r$, where r_0 is the first iteration after convergence is reached, R is the total number of iterations and λ_k^r is the sample value of λ_k in the r -th iteration.

If the LC-MS data also contain MS2 fragmentation spectra, then MS1 detected peptides can be linked to MS2 identified features given by software such as SEQUEST to obtain peptide sequence information.

3 RESULTS AND DISCUSSION

We report the observed performance of BPDA2d, side by side with state-of-the-art methods, such as msInspect and BPDA in a number of experiments using both synthetic and real data. The efficiency of BPDA2d in detecting low abundance and overlapping peptides is illustrated.

3.1 Results for synthetic data

3.1.1 Synthetic 100-mix LC–MS datasets with different abundance levels (SNRs) First, to test robustness of various algorithms, we generated LC–MS datasets with different signal to noise ratios (SNRs) using methods described by Schulz-Trieglaff *et al.* More specifically, the mean signal strength (peptide abundance) was varied while the noise level (mean and variance of noise) was fixed. For each peptide abundance level $a \in \{100, 500, 5000\}$, the simulation was repeated 30 times. In each repetition, 100 true peptides (with abundance level a and masses randomly selected from tryptic digested human proteins) served as inputs of the model given by Equation (4). The charge state distribution of one peptide was modeled by a binomial distribution, which was reported to approximate the real data well (Schulz-Trieglaff *et al.*, 2008). The isotopic distribution was calculated theoretically based on peptide sequence. The peptide elution profile was modeled by an exponentially modified Gaussian distribution, which captures different distortions of elution peaks by considering tailing and fronting effects (Di Marco *et al.*, 2001). Each output dataset consists of 100 MS spectra with mass resolution 15 000.

BPDA2d, BPDA and msInspect (the latest Build 613) were applied to the same datasets to give detection results. We mainly focus on the performance comparison between BPDA2d and its precursor BPDA, which was shown to outperform popular algorithms such as OpenMS (Version 1.6.0), Decon2LS and VIPER in Sun *et al.* (2010). We also include msInspect in the comparison since it is widely used and has been reported to outperform other algorithms (Zhang *et al.*, 2009) such as MZmine. To apply BPDA, we followed the procedure introduced in the original paper (Sun *et al.*, 2010): peptide elution peaks were first detected along the RT dimension, and elution peaks with similar RT were grouped. Each group contains a series of consecutive spectra, which were then averaged to form a mean spectrum. Each mean spectrum was analyzed by BPDA, and finally an overall feature list was produced. To apply msInspect, we first wrote each simulated dataset into a text file with three columns specified by RT, m/z and intensity. Next, the text file was converted to mzXML and then msInspect was applied to give detection results including detected features and their qualities. The input parameters of msInspect were set to enable the inclusion of as many reasonable features as possible ('minpeaks' and 'maxkl' were set to 2 and 10, respectively).

When comparing BPDA2d to its precursor BPDA, we found that the former had several advantages over the latter as detailed below. (i) For each experiment conducted, the total number of candidates considered in BPDA2d was greatly reduced compared with BPDA (reduced by 43% on average). This is expected since BPDA2d imposes additional constraints on candidates' elution peaks and can preclude non-reproducible noise peaks from the candidate list. To clarify, BPDA2d searches for candidates which can be repetitively observed across retention time—i.e. candidates whose elution peaks can be clearly identified. Thus, a major fraction of noise peaks (e.g. shot noise) which are not reproducible in time is removed. In contrast, BPDA is a 1D algorithm which works along the m/z dimension and processes one mean scan at a time. The mean scan is produced by taking the average of a few consecutive spectra. Thus, although noise in the form of random intensity fluctuation can be canceled out to some degree, non-reproducible noise peaks are still likely to be included in the resulting mean

scan and therefore in the candidate list. Also, BPDA is likely to split long elution peaks into multiple mean scans and thus generate multiple candidates for a single true peptide. In summary, BPDA2d can compile a more reliable candidate list, which may help to reduce the number of detected false positives (FPs), and can allocate limited computational resources to candidates more likely to be true positives (TPs).

(ii) BPDA2d reported significantly fewer FPs with existence probability >0.9 than BPDA (reduced by 47% on average) and detected more TPs than the latter (increased by 6% on average). This improvement of BPDA2d is achieved by taking into account peptide elution peaks in addition to isotopic distribution and charge station distribution. BPDA2d tries to use all available observations from possible positions on the m/z -RT plane to infer the overall signal of each peptide candidate. By utilizing more information, detected signals become more reliable and the evidence of candidates' existence or non-existence becomes stronger, resulting in better detection results in terms of more TPs and less FPs.

When comparing BPDA2d to msInspect, we found that on average the TPs detected by BPDA2d increased by 16% with respect to the latter while the FPs reduced by 40% (quality thresholds were set to existence probability >0.9 and KL <1 , for the two algorithms, respectively).

To give a complete picture of the detection results, the classic precision–recall (PR) curve has been adopted to evaluate the performance of various algorithms since the ground truth of the data is known. To obtain the PR curve, first a series of detection levels was selected, which range from the lower bound to the upper bound of feature quality scores (i.e. existence probability for BPDA and BPDA2d; KL score for msInspect). Features with quality score better than a given detection level were said to be detected at this specific detection level. A detected feature was claimed to be a true positive if it had the correct monoisotopic mass (e.g. within 10 ppm of the true mass), the correct RT (with a 6-scan tolerance), and the true RT is within the boundaries of the feature's elution peak; otherwise, the detected feature was called a false positive. Then, the true positive rate (TPR, i.e. recall) and precision (Prec) were calculated at each detection level as follows: $TPR = \frac{TruePositive}{TruePositive + FalseNegative}$ and $Prec = \frac{TruePositive}{TruePositive + FalsePositive}$. The average PR curve for one abundance level was then obtained (each point on the curve was a pair of average precision and TPR at one detection level for all repetitions). We found that the PR results were largely influenced by the size of the mass window used for matching detected features with the list of true peptides. PR curves for various mass windows are shown in Figure 1.

In the PR space, the upper right corner (with coordinate [1,1]) represents 100% sensitivity (no false negatives) and 100% precision (no false positives). The closer the PR curve is to the upper right corner, the better the algorithm. In this sense, BPDA2d is generally the best among all methods at all abundance levels. BPDA2d's performance is the least affected by the deterioration of SNRs among the three algorithms. Thus, BPDA2d provides the most robust performance for lower abundance peptides.

Another advantage of BPDA2d is that it has much higher reported mass accuracy. In the Supplementary Material, we provide comparison of mass accuracies of all three algorithms, and we have shown that the mass accuracy reported by BPDA2d is significantly higher than the other two algorithms. Given different

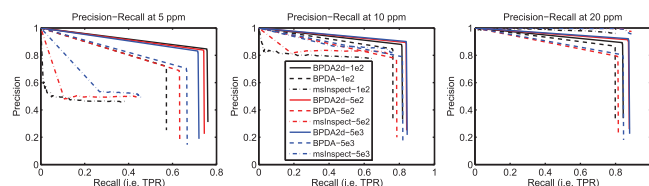


Fig. 1. PR results for synthetic LC-MS datasets with different abundance levels (SNRs). Each panel shows the results obtained at a different mass window size as suggested by the title. Color codes for different abundance levels. Each method is represented by a unique line type. BPDA2d renders the best precision and sensitivity (i.e. recall) among all the methods compared for all abundance level in the first two mass window cases. In the last case, the performance between BPDA2d and msInspect has a very small difference.

mass accuracies, there is not a fair way for performance evaluation. Thus, we provide performance evaluation in three cases when different mass window sizes are used. It can be seen that the mass window size does not affect the performance of BPDA2d significantly after 10 ppm because of its high mass accuracy. On the other hand, msInspect deteriorates quickly as we narrow the mass window from 20 to 10 ppm due to its low mass accuracy. BPDA2d outperforms msInspect at higher mass accuracies of 10 and 5 ppm. In the case of 20 ppm, given the simple composition of the simulated data, the performance between BPDA2d and msInspect is similar. It shall be noted that with different mass accuracies by different algorithms, sample composition will strongly affect the reported PR curve—if the sample is more complex, with more peptides of similar weights, then an algorithm with lower mass accuracy like msInspect will further deteriorate in performance.

3.1.2 Synthetic LC-MS dataset with eight pairs of overlapping peptides As noted, overlapping peptide peaks can complicate mass spectra and make the detection problem much harder. Hence, it is important to investigate algorithm performance in the presence of overlapping peptides. A synthetic 16-peptide-mix was generated by eight pairs of overlapping tryptic digested human peptides. The dataset contains 1000 LC-MS spectra with mass resolution 15 000. The intensity ratio of each pair (light/heavy) ranges from 0.25 to 3, and peptide charge states range from 1 to 4. More details on these peptides and the detection results of different algorithms are summarized in Table 1.

For the first 4 pairs, the challenges are mainly to detect and split overlapping elution peaks of the two peptides in each pair with similar weights and close RT. For instance, the elution profiles and observed signals of the two peptides in the first pair are shown in Figure 2. We observe that the two peptides have significant overlapping signal regions, which makes the detection problem tough. MsInspect experienced difficulty in identifying this pair. In fact, it failed to split the overlapping elution peaks and treated the two peptides as a single one. As a result, the intensity of the reported peptide (the second one) equals the total intensity of the two. For BPDA, although it could report both peptides correctly, the intensity results were inaccurate (the intensity ratio turned out to be >1 while the true ratio was 0.67). BPDA detected the second peptide correctly from 106s to 128s (approximately from the beginning to the maximum of the second peptide's elution profile, see Fig. 2a), while the rest of the signal peaks which appeared after 128s were shadowed by the first peptide, whose signal was stronger. Therefore,

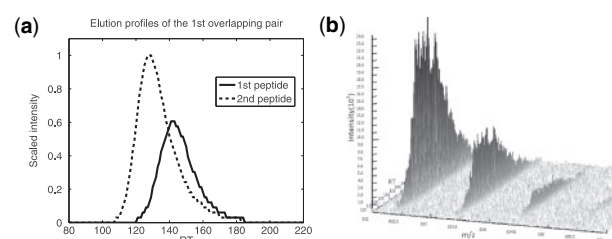


Fig. 2. Overlapping signals of the first pair in 16-mix. (a) Overlapping LC profiles of the two peptides. (b) Signal peaks of the two peptides at charge state 1 in a 3D view. SNR at this region is quite low, and significant peak overlapping can be observed.

in this region BPDA failed to include the second peptide in its candidate list and tried to use the first peptide alone to explain the observed signal. The second peptide's corresponding intensity was thus wrongly attributed to the first one, thereby leading to inaccurate intensity results. In contrast to msInspect and BPDA, BPDA2d correctly split the elution peaks of the two peptides by capturing the tiny mass difference of the two and by detecting intensity dips in the observed overlapping peaks.

For the last four pairs, the weights of two peptides in each pair differ approximately by a multiple of the neutron weight. As a result, their isotopic peaks overlap at different isotope numbers and the overall isotope pattern deviates from each individual's. Thus, it is more challenging to utilize individual isotope pattern to discern the overlapping pair. As a vivid example, the elution profiles and the observed signals of peptides in the sixth pair are shown in Figure 3. It is observed that the SNR at corresponding regions was quite high and peaks of the second peptide in this pair almost got completely shadowed under all but the first isotope peak of the first peptide (Fig. 3a and b). Hence, the overall signal pattern (Fig. 3c) deviates from each individual's isotope pattern (Fig. 3d). MsInspect was not able to detect this deviation: the calculated KL distance between the overlapping peak cluster and the first peptide's theoretical isotope pattern was surprisingly small (~ 0.027), suggesting a 'good' match by its own criterion (a smaller KL score suggests a better match). MsInspect thus stopped there and assigned all overlapping signals to the first peptide, failing to consider the second peptide. This failure was not caused by chance. In fact, for the last four pairs, msInspect could correctly detect only one pair of peptides (the one with the least overlap) and missed one peptide in each of the other three pairs. This illustrates the inefficiency of template matching algorithms such as msInspect in dealing with overlapping isotope patterns as compared with BPDA2d and BPDA. Indeed, one should be wary of taking KL distance, or other distance measures adopted by template matching algorithms, as a reliable measurement of the isotope pattern deviation. BPDA proposed a candidate corresponding to the second peptide; however, the candidate's existence probability was inferred to be 0, thereby rendering it undetectable. This was caused by the penalty term adopted in BPDA that penalizes model complexity. More specifically, the additional inclusion of the second peptide could reduce the MSE between the observed and inferred peaks to a small extent, but this reduction in MSE could not beat the increase of model complexity. Therefore, BPDA inferred the second peptide to be non-existent. Although BPDA2d utilizes a similar penalty strategy, the penalty term did not cause exclusion of the second peptide because BPDA2d used more observations from

Table 1. Results of the dataset with eight pairs of overlapping peptides

Pair no.	Sequence	True peptide info				BPDA2d		BPDA		msInspect	
		Mass(Da)	RT(s)	CS	Intn	CS	Intn	CS	Intn	CS	Intn
1	DYSYER	831.34	141	1–2	0.0004	1–2	0.0003	1–2	0.0008	NA	
	DENGELR	831.37	127	1–2	0.0006	1–2	0.0006	1–2	0.0005	1–2	0.001
2	VVFMSLCK	925.48	414	1–2	0.0046	1–2	0.0033	1–2	0.0043	1–2	0.0050
	LLLPCLVR	925.58	456	1–2	0.0054	1–2	0.0044	1–2	0.0056	1–2	0.0068
3	MTPELMIK	961.50	323	1–3	0.0001	1–3	0.0001	1–3	0.0001	1–2	0.0001
	IAVMLMER	961.51	340	1–3	0.0002	1–3	0.0002	1–3	0.0003	1–3	0.0003
4	ACCLLCGCPK	1009.42	302	1–3	0.0011	1–3	0.0008	1–3	0.0023	1–3	0.0024
	MLCAGIMSGK	1009.48	314	1–3	0.0008	1–3	0.0009	1–3	0.0014	1–3	0.0020
5	AYDPDYER	1027.42	174	1–3	0.0077	1–3	0.0078	1–3	0.0081	NA	
	EETSGDGELP	1028.43	194	1–3	0.0307	1–3	0.0344	1–3	0.0418	1–3	0.0382
6	NGNEEGEER	1032.41	75	1–3	0.4612	1–3	0.5110	1–3	0.7140	1–3	0.7284
	TEGEEDAQR	1033.43	79	1–3	0.1537	1–3	0.1065	NA		NA	
7	MLANLVMHK	1055.56	312	1–3	0.0019	1–3	0.0018	1–3	0.0017	1–3	0.0023
	LTLDLMKPK	1057.62	321	1–3	0.0009	1–3	0.0010	1–3	0.0008	NA	
8	LLPPLLQIVCK	1235.77	561	1–4	0.1768	1–4	0.1755	1–4	0.1405	1–4	0.1193
	LMLFMLAMNR	1238.63	577	1–4	0.1537	1–4	0.1516	1–4	0.0779	1–4	0.0943

CS and Intn denote detectable charge states and normalized intensity, respectively.

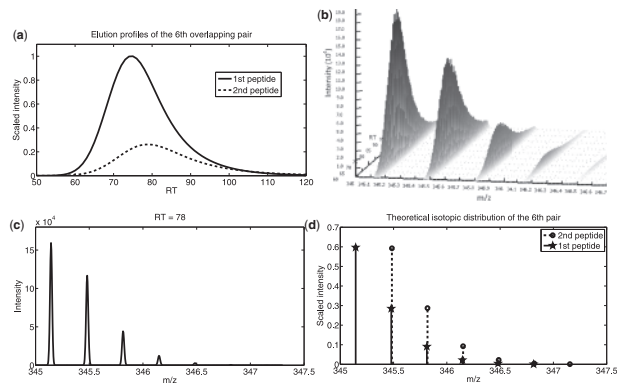


Fig. 3. Overlapping signals of the sixth pair in 16-mix. (a) Overlapping LC profiles. (b) Signal peaks of the two peptides at charge state 3 in a 3D view. This region has a high SNR, where peaks of the second peptide almost get completely shadowed by all but the first isotope peak of the first peptide. (c) MS scan sampled at 78s showing signals of the same pair. The observed overall signal pattern deviates from (d) theoretic isotope patterns of the two peptides.

the m/z -RT plane than BPDA and the improvement in fitting the observed signal by inclusion of the second peptide was significant, thereby offsetting the penalty.

In summary, BPDA2d correctly detected all 46 charge states of the 16 peptides (along with 16 FPs), while BPDA and msInspect correctly detected 43 and 34 charge states, along with 57 and 4 FPs, respectively (See the Supplementary Material for more details). All detected TPs of BPDA2d and BPDA had existence probability equaling to 1. For msInspect, the KL scores of TPs were <0.76. The box plots of mass and intensity deviation results given by the three algorithms are shown in Figure 4. We observe that among the three algorithms, on average BPDA2d gave the most accurate abundance results and msInspect’s results were the least accurate.

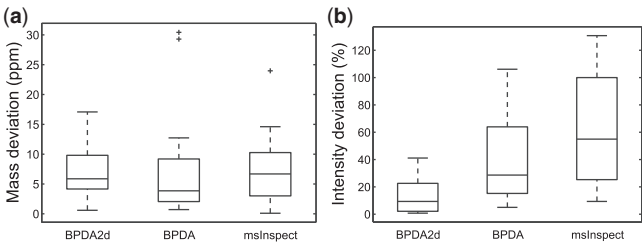


Fig. 4. Box plots of (a) absolute mass deviation and (b) normalized intensity deviation of BPDA2d, BPDA and msInspect for the 16-mix dataset.

BPDA had the best mass accuracy evaluated by the median mass deviation, but it rendered a few outliers and a larger variance compared with BPDA2d. Overall, msInspect produced the least accurate mass results. The synthetic test data are available upon request.

3.2 Results for real data

3.2.1 Data preparation A QTOF LC–MS/MS dataset was downloaded from the repository of the Seattle Proteome Center that is provided as a standard for testing algorithms. The dataset was collected on a Waters/Micromass (Milford, MA, USA) Q-TOF Ultima with Agilent 1100 series autosampler, Agilent 1100 series nanopump flowing at 200 nl/min and electrospray ionization. Approximately 200 fmol of total protein was injected on-column. The dataset contains over 3500 MS1 spectra (m/z ranges from 250 to 1400 with FWHH ~0.15 Da) and 775 MS2 spectra generated by peptides from 18 tryptic digested proteins (obtained from Bovine, Rabbit, Horse, etc.). More details can be found in (Klimek *et al.*, 2008). MS1 level peptide detection was performed using BPDA2d, BPDA, and msInspect (the latest Build 613). We tried to optimize input parameters for msInspect: ‘minpeaks’ was set to 2 and ‘maxkl’ was set to 10, enabling the inclusion of as many reasonable

features as possible. The ‘walksmooth’ option was selected as it was recommended for QTOF data and improved the performance. For BPDA, post-processing was applied to combine features that were split over consecutive mean spectra.

3.2.2 Comparative results Direct comparison of results across different methods is meaningless unless ground truth of the data is known, but owing to contaminants and issue of peptide detectability, the true data composition is hard to know. As a workaround, SEQUEST and PeptideProphet were applied to analyze all the acquired MS2 spectra, rendering 234 unique peptide identifications associated with a high probability score (i.e. PeptideProphet score >0.9) and could somehow reveal a portion of the truly existing peptides in the sample. We thus compared the detection results given by aforementioned MS1-based methods to the MS2 identifications. We say a MS1 feature is matched to a MS2 feature if the RT of the MS2 feature is within the retention peak of the MS1 feature and the mass deviation is within 40 ppm. The size of the mass window is chosen to include as many good matches as possible. It is larger than that used for synthetic data since here the ground truth peptide weights are unknown, and mass errors are associated with MS2 identifications as well as MS1 features. MS1 identifications were first filtered based on mass and RT. Only features with mass 1000–3710 Da and RT in the range of 840–2030 scan were considered since all MS2 identifications were from these ranges. Remaining features were then selected based on the reported quality score. Because schemes for calculating feature quality score vary across different algorithms, to ensure a fair and meaningful comparison, quality cutoff thresholds for various algorithms were carefully chosen as detailed below so that they corresponded to the same significant level.

- For BPDA2d and BPDA, existence probabilities are employed to measure feature quality. The cutoff thresholds of existence probability were calculated based on its null distribution, i.e. the distribution of existence probability of those candidates that are non-existing in the sample. We identify these peptides as those highly correlated (i.e. can be grouped into the same cluster as described in Section 2) with one of the candidates that can be matched to the MS2 identification list. Although the ground truth is unknown, the latter candidates are likely to be TPs as they are confirmed by the MS2 identifications with high reliability, while the former are false identifications co-existing with the latter. These co-existing candidates should be assigned with a low existence probability. Given a significant level α , the corresponding threshold γ of the existence probability P can be calculated based on the right-tail probability of the null distribution: $\{\gamma | \text{Prob}(P \geq \gamma) = \alpha\}$.
- MsInspect uses KL score to measure feature quality. Cutoff KL thresholds were selected based on KL null distribution, i.e. the distribution of KL scores calculated between random noise and authentic isotopic distributions, as described by Haskins *et al.* (2011). If KL score can faithfully reflect the deviation between random noise and real isotopic patterns, then the KL null distribution should skew to the right or have a small left-tail probability. On the other hand, given a significant level α , the corresponding KL threshold τ could be calculated based on the left-tail probability: $\{\tau | \text{Prob}(KL \leq \tau) = \alpha\}$.

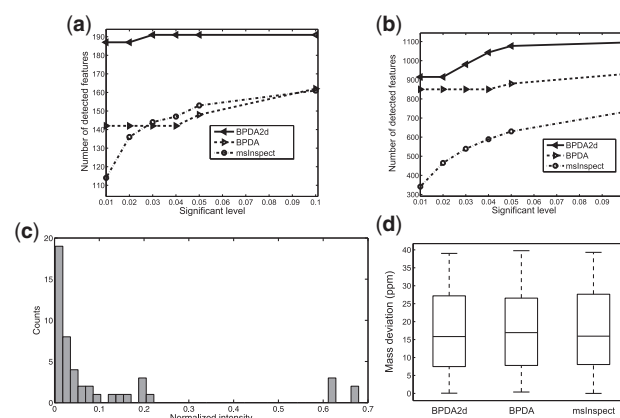


Fig. 5. Detection results of the QTOF LC-MS/MS dataset. BPDA2d, BPDA and msInspect detected (a) total number of features and (b) number of features that can be matched to MS2 identifications at various significant levels. At significant level 0.05, the following two panels are obtained: (c) Histogram of normalized intensity of features detected by BPDA2d but not msInspect. Most of the features are from the low intensity region. (d) Box plots of absolute mass deviation of different algorithms.

From Figure 5a, it can be seen that BPDA2d detected many more features from the MS2 list than BPDA and msInspect at each significant level compared. Improvements are from 32% to 18%, and 64% to 19% compared to BPDA and msInspect, respectively, when significance level increases from 0.01 to 0.1, indicating a 3- to 6-fold increase in peptide coverage and quantification. In addition, all three MS1-based algorithms detected significantly more features than that covered by the 234 MS2 identifications (Fig. 5b), illustrating the under-sampling problem of MS2 and highlighting the benefits of employing MS1-based peptide detection algorithms to improve protein coverage rate. Performances of various algorithms were further investigated at a 0.05 significance level. The histogram of normalized intensity of MS2-level identifications detected by BPDA2d but not by msInspect is plotted in Figure 5c. The majority of identifications detected only by BPDA2d concentrate at the low intensity region (i.e. the area with normalized intensity <0.1), illustrating that BPDA2d can better identify low abundance peptides than msInspect. In addition, extra identifications yielded by BPDA2d did not cause degradation in mass accuracy (Fig. 5d). Moreover, BPDA2d slightly beat the other two methods in terms that the mean mass deviation is reduced by ~2%. The average computational time of BPDA2d, BPDA and msInspect for testing datasets are 3.5 h, 1 h and 2.2 min, respectively (see the Supplementary Material for more details). BPDA2d is expected to be more time-consuming since it looks for the optimal solution iteratively through Gibbs sampling on the whole spectra, while greedy template matching-based algorithms work on one local region at a time and calculate the fitting score, which typically does not require much computation. But we point out that the BPDA2D algorithm is fully parallelizable, and the authors are in fact working on a parallel version of the software that will be much faster.

4 CONCLUSION

We have presented BPDA2d, a global optimization-based Bayesian peptide detection algorithm for LC-MS data. Feature extraction

from LC–MS data is complicated by several factors such as protein wide dynamic range, high signal density and variability of liquid chromatography. BPDA2d is designed to tackle these problems. It extracts all pertinent observations (including isotope pattern, charge state distribution and LC elution peaks) and pieces all evidence together for the detection of each candidate, blending information to better identify weak peptide signals. Based on a rigorous statistical framework, BPDA2d optimizes all candidates' signals globally, resulting in more effective detection of overlapping peptides compared with local template matching-based methods that detect peptides one by one in a greedy manner. Instead of employing pre-assumed elution peak models, BPDA2d derives peptide elution profiles directly from observations. Therefore, it is more robust in dealing with LC fluctuations and more adaptable across analysis platforms.

We have shown that BPDA2d performs well on both simulated data and real data for various signal to noise ratios and in complex cases where features overlap. Our experimental results indicate that BPDA2d outperforms state-of-the-art software such as msInspect and BPDA in terms of sensitivity and detection accuracy. As the mass resolution and accuracy of MS instruments continue to improve, we expect BPDA2d to achieve better qualification and quantification results. We think the main application of BPDA2d will be on TOF instruments, which suit our data model better. BPDA2d is publicly available and we hope it will be useful to the wider community.

Funding: The authors thank the support of the Partnership for Personalized Medicine (PPM) project, through Translational Genomics (TGen) contract C08-00904. J.Z.'s work is supported by a grant from the National Institutes of Health (NIH2G12RR013646-11).

Conflict of Interest: none declared.

REFERENCES

- Bantscheff, M. et al. (2007) Quantitative mass spectrometry in proteomics: a critical review. *Anal. Bioanal. Chem.*, **389**, 1017–1031.
- Bellew, M. et al. (2006) A suite of algorithms for the comprehensive analysis of complex protein mixtures using high-resolution LC-MS. *Bioinformatics*, **22**, 1902–1909.
- Cox, J. et al. (2008) Maxquant enables high peptide identification rates, individualized p.p.b-range mass accuracies and proteome-wide protein quantification. *Nat. Biotechnol.*, **26**, 1367–1372.
- Di Marco, V.B. et al. (2001) Mathematical functions for the representation of chromatographic peaks. *J. Chromatogr. A*, **931**, 1–30.
- Dijkstra, M. et al. (2009) Optimal analysis of complex protein mass spectra. *Proteomics*, **9**, 3869–3876.
- Domon, B. et al. (2006) Mass spectrometry and protein analysis. *Science*, **312**, 212.
- Frank, R. et al. (2003) Clinical biomarkers in drug discovery and development. *Nat. Rev. Drug Discov.*, **2**, 566–580.
- Geman, S. et al. (1984) Stochastic relaxation, gibbs distributions, and the bayesian restoration of images. *IEEE Trans. Pattern Anal. Mach. Intell.*, **6**, 721–741.
- Haskins, W.E. et al. (2011) MRCQuant- an accurate lc-ms relative isotopic quantification algorithm on tof instruments. *BMC Bioinformatics*, **12**, 74.
- Hoopmann, M.R. et al. (2007) High speed data reduction, feature selection, and MS/MS spectrum quality assessment of shotgun proteomics datasets using high resolution mass spectrometry. *Anal. Chem.*, **79**, 5630–5632.
- Jaitly, N. et al. (2009) Decon2ls: an open-source software package for automated processing and visualization of high resolution mass spectrometry data. *BMC Bioinformatics*, **10**, 87.
- Katajamaa, M. et al. (2005) Processing methods for differential analysis of lc/ms profile data. *BMC Bioinformatics*, **6**, 179.
- Keller, A. et al. (2002) Empirical statistical model to estimate the accuracy of peptide identifications made by ms/ms and database search. *Anal. Chem.*, **74**, 5383–5392.
- Klimek, J. et al. (2008) The standard protein mix database: a diverse dataset to assist in the production of improved peptide and protein identification software tools. *J. Proteome Res.*, **7**, 96.
- Leptos, K.C. et al. (2006) MapQuant: open-source software for large-scale protein quantification. *Proteomics*, **6**, 1770–1782.
- Li, X. et al. (2005) A software suite for the generation and comparison of peptide arrays from sets of data collected by liquid chromatography-mass spectrometry. *Mol. Cell Proteomics*, **4**, 1328–1340.
- Monroe, M.E. et al. (2007) VIPER: an advanced software package to support high-throughput LC-MS peptide identification. *Bioinformatics*, **23**, 2021–2023.
- Morris, J.S. et al. (2005) Feature extraction and quantification for mass spectrometry in biomedical applications using the mean spectrum. *Bioinformatics*, **21**, 1764–1775.
- Mueller, M. et al. (2007) Superhirn-a novel tool for high resolution LC-MS based peptide/protein profiling. *Proteomics*, **7**, 3470–3480.
- Nesvizhskii, A.I. et al. (2006) Dynamic spectrum quality assessment and iterative computational analysis of shotgun proteomic data: toward more efficient identification of post-translational modifications, sequence polymorphisms, and novel peptides. *Mol. Cell. Proteomics*, **5**, 652–670.
- Perkins, D.N. et al. (1999) Probability-based protein identification by searching sequence databases using mass spectrometry data. *Electrophoresis*, **20**, 3551–3567.
- Renard, B.Y. et al. (2008) NITPICK: peak identification for mass spectrometry data. *BMC Bioinformatics*, **9**, 355.
- Robert, C.P. et al. (2004) *Monte Carlo Statistical Methods*. Springer, New York.
- Rockwood, A.L. et al. (1995) Rapid calculation of isotope distributions. *Anal. Chem.*, **67**, 2699–2704.
- Schulz-Trieglaf, O. et al. (2008) Lc-MSsim – a simulation software for liquid chromatography mass spectrometry data. *BMC Bioinformatics*, **9**, 423.
- Schwarz, G. (1978) Estimating the dimension of a model. *Ann. Stat.*, **6**, 461–464.
- Senko, M.W. et al. (1995) Determination of monoisotopic masses and ion populations for large biomolecules from resolved isotopic distributions. *J. Am. Soc. Mass Spectrom.*, **6**, 229–233.
- Sturm, M. et al. (2008) Openms – an open-source software framework for mass spectrometry. *BMC Bioinformatics*, **9**, 163.
- Sun, Y. et al. (2010) BPDA – a Bayesian peptide detection algorithm for mass spectrometry. *BMC Bioinformatics*, **11**, 490.
- Zhang, J. et al. (2009) Review of peak detection algorithms in liquid-chromatography-mass spectrometry. *Curr. Genomics*, **10**, 388–401.